

Human in Events: A Large-Scale Benchmark for Human-centric Video Analysis in Complex Events

Weiyao Lin, Huabin Liu, Shizhan Liu, Yuxi Li, Rui Qian, Tao Wang, Ning Xu
Hongkai Xiong, Guo-Jun Qi and Nicu Sebe

Abstract—Along with the development of modern smart cities, human-centric video analysis has been encountering the challenge of analyzing diverse and complex events in real scenes. A complex event relates to dense crowds, anomalous, or collective behaviors. However, limited by the scale of existing video datasets, few human analysis approaches have reported their performance on such complex events. To this end, we present a new large-scale dataset, named Human-in-Events or HiEve (Human-centric video analysis in complex Events), for the understanding of human motions, poses, and actions in a variety of realistic events, especially in crowd and complex events. It contains a record number of poses (>1M), the largest number of action instances (>56k) under complex events, as well as one of the largest numbers of trajectories lasting for longer time (with an average trajectory length of >480 frames). Based on this dataset, we present an enhanced pose estimation baseline by utilizing the potential of action information to guide the learning of more powerful 2D pose features. We demonstrate that the proposed method is able to boost the performance of existing pose estimation pipelines on our HiEve dataset. Furthermore, we conduct extensive experiments to benchmark recent video analysis approaches together with our baseline methods, demonstrating that HiEve is a challenging dataset for human-centric video analysis. We expect that the dataset will advance the development of cutting-edge techniques in human-centric analysis and the understanding of complex events. The dataset is available at <http://humanevents.org>.

Index Terms—complex events, human-centric analysis, datasets



1 INTRODUCTION

THE development of smart cities highly relies on the advancement of fast and accurate visual understanding of multimedia. To achieve this goal, many human-centered and event-driven visual understanding problems have been raised, such as human pose estimation [9], pedestrian tracking [6], and action recognition [10], [11].

Recently, several public datasets (e.g., MSCOCO [1], PoseTrack [4], UCF-Crime [8]) have been proposed to benchmark the aforementioned tasks. However, they have some limitations when applied to real scenarios with complex events such as dining, earthquake escape, subway getting-off and collisions. *First*, most benchmarks focus on normal or relatively simple scenes. These scenes either have few occlusions or contain many easily-predictable motions and poses. *Second*, the coverage and scale of existing benchmarks are still limited. For example, although the UCF-Crime dataset [8] contains challenging scenes, it only has coarse video-level action labels which may not be enough for fine-grained action recognition. Similarly, although the numbers of pose labels in MSCOCO [1] and PoseTrack [4]

are sufficiently large for simple scenes with limited occlusions, these datasets lack realistic scenes containing crowded scenes and complex events.

To this end, we present a new large-scale human-centric dataset, named Human-in-Events (HiEve), for understanding a hierarchy of human-centric information (motions, poses, and actions) in a variety of realistic complex events, especially in crowded and complex events. Among all datasets for realistic crowd scenarios, HiEve has substantially larger scales and complexity and contains a record number of poses (>1M), action labels (>56k) and long trajectories (with average trajectory length >480 frames). Compared with existing datasets, HiEve contains more comprehensive and larger-scale annotations in more complex scenes, making it more adequate to develop new human-centric analysis techniques and evaluate them in realistic scenes. Table 1 provides a quantitative comparison of the HiEve dataset with related datasets in light of their nature and scale.

One main feature of our HiEve dataset is the hierarchical and diverse information of human annotations. To sufficiently utilize this feature, we present an action-guided pose estimation algorithm as our baseline method, which guides the pose representation learning with additional action-aware information. Experiments demonstrate that this action-guided design is able to boost the performance of existing state-of-the-art pipelines on our HiEve dataset.

Additionally, we build an online evaluation server available to the whole community in order to enable timely and scalable evaluation on the held-out test videos. We

- W. Lin, H. Liu, S. Liu, Y. Li, R. Qian, W. Tao and H. Xiong are with the Department of Electronic Engineering, Shanghai Jiao Tong University, China (email: {wylin, huabinliu, shanluzuode, lyxok1, qru9911, wang_tao1111, xionghongkai}@sjtu.edu.cn).
- N. Xu is with Adobe Research, USA (email: nxu@adobe.com).
- G. Qi is with the Machine Perception and Learning Lab, USA (email: guojunq@gmail.com).
- N. Sebe is with the University of Trento, Trento, Italy (email: niculae.sebe@unitn.it).

Table 1: Comparison between HiEve and existing datasets. “NA” indicates not available. “~” denotes approximated value. “traj.” means trajectory and “avg” indicates average trajectory length.

Dataset	# pose	# box	# traj.(avg)	# action	pose track	surveillance	complex events
MSCOCO [1]	105,698	105,698	NA	NA	×	×	×
MPII [2]	14,993	14,993	NA	410	×	×	×
CrowdPose [3]	~80,000	~80,000	NA	NA	×	×	×
PoseTrack [4]	~267,000	~26,000	5,245(49)	NA	✓	×	×
MOT16[5]	NA	292,733	1,276(229)	NA	×	✓	×
MOT17	NA	901,119	3,993(226)	NA	×	✓	×
MOT20 [6]	NA	1,652,040	3457(478)	NA	×	✓	×
Avenue [7]	NA	NA	NA	15	×	✓	×
UCF-Crime [8]	NA	NA	NA	1,900	×	✓	✓
HiEve (Ours)	1,099,357	1,302,481	2,687(485)	56,643	✓	✓	✓

also evaluate existing state-of-the-art solutions on HiEve to benchmark their performance and analyze the corresponding oracle models, demonstrating that HiEve is challenging and of great value for advancing human-centric video analysis.

2 RELATED WORKS AND COMPARISON

2.1 Multi-object Tracking Datasets

Different from single-object tracking, multi-object tracking (MOT) does not solely depend on sophisticated appearance models to track objects in frames. In recent years, there is a corpus of datasets that provide multi-object bounding-box and track annotations in video sequences, which have fostered the development of this field. PETS [12] is an early proposed multi-sensor video dataset, it includes annotation of crowd person count and tracking of an individual within a crowd. Its sequences are all shot in the same scene, which leads to relatively simple samples. KITTI [13] tracking dataset features videos from a vehicle-mounted camera and focuses on street scenarios, it owns 2D & 3D bounding-boxes and tracklets annotations. Meanwhile, it has a limited variety of video angles. The most popular benchmark to data for the evaluation of tracking is the MOT-Challenge [6], which shows pedestrians from a variety of different viewpoints. However, with the rapid development of MOT algorithms and the limitation of scale and complexity of the MOT-Challenge dataset, it is less suitable for a comprehensive and general benchmark on tracking performance of each method on complex scenarios of the real world.

2.2 Pose Estimation and Tracking Datasets

Human pose estimation in images has made great progress over the last few years. For single-person pose estimation, LSP [14], FLIC [15] are the two most representative benchmarks, the former focuses on sports scenes while the latter is collected from popular Hollywood movie sequences. Compared with LSP, FLIC only labels 10 upper body joints and owns a smaller data scale. WAF [16] is the first to establish a benchmark for multi-person pose estimation with simplified keypoint and body definition. Then, MPII [2] and MSCOCO [1] datasets were proposed to further advance the multi-person pose estimation task by their diversity and difficulty in the human pose. In particular, MSCOCO is regarded as the most widely used large-scale dataset with 105698 pose annotations in hundreds of daily activities. Taking the tracking task into consideration, PoseTrack [4]

builds a new video dataset which provides multi-person pose estimation and articulated tracking annotations. Similar to PoseTrack, JAT [17], a recently proposed massive CG dataset, simulates realistic urban scenarios for human pose estimation and tracking.

2.3 Action Recognition Datasets

There are two human action video datasets that have emerged as standard benchmarks for action recognition task: HMDB-51 [18] and UCF-101 [19]. HMDB-51 is mainly collected from movie sequences and contains 51 action categories. UCF-101 is one of the datasets with the largest number of action categories (101 classes) and samples, which significantly promote the development of action recognition task. Aimed to recognize the realistic anomalous behavior, Avenue [7] and UCF-Crime [8] are proposed. UCF-Crime annotates 13 anomalies in real-world surveillance videos, such as fighting, accident and robbery. Recently, Kinetics [20] and AVA [21] datasets with larger scale and detailed object information are constructed to facilitate the advancement and evaluation on video analysis techniques. However, most of the contents in these videos are collected from either drama scenes or uncrowded scenarios.

2.4 Comparisons

The related datasets mentioned above have served the community very well, but now they are confronting several limitations: (1) Most of them are focusing on normal or simple scenes (e.g. street, sports scene, single-person movement), which owns few occlusions and is relatively simple for the prediction of motions or poses. (2) Their coverage and scales are less useful to the evaluation of the state-of-the-art algorithms. (3) Multiple human-centric video analysis tasks need to learn and evaluate on multiple benchmarks while annotations from previous datasets only contain a single aspect of human information (pose, track or action). Overall, compared with these datasets, our dataset has the following unique characteristics:

- HiEve dataset covers a wide range of human-centric understanding tasks including motion, pose, and action, while the previous datasets only focus on a subset of our tasks.
- HiEve dataset has substantially larger data scales, including the currently largest number of poses (>1M), the largest number of complex-event action labels (>56k), and one of the largest number of trajectories with long terms (with average trajectory length >480).



Figure 1: Samples of different actions from our training set and testing set.

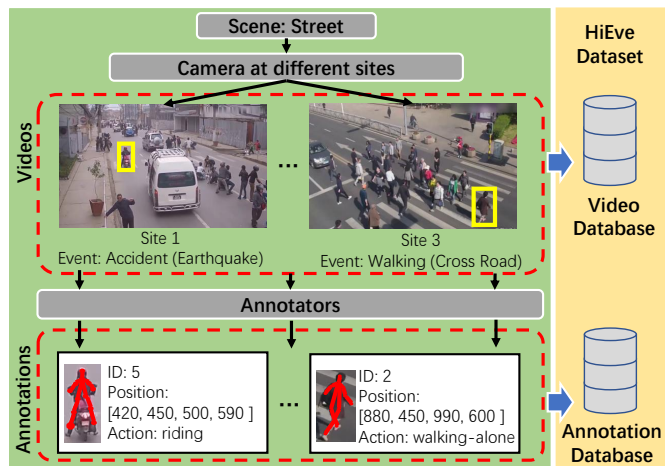


Figure 2: An example of the collection workflow of our HiEve dataset for the street scene; each scene contains videos captured at different sites with different types of events happening.

- HiEve dataset focuses on the challenging scenes under various crowded and complex events (such as dining, earthquake escape, subway getting-off, and collision), while the previous datasets are mostly related to normal or relatively simple scenes.

In a nutshell, our HiEve contains more comprehensive and larger-scale annotations in various complex-event scenes, making it more capable of evaluating the human-centric analyzing techniques in realistic scenes.

3 THE HIEVE DATASET

3.1 Collection and Annotation

Collection. We start by selecting several crowded places with complex and diverse events for video collection. In total, our video sequences are collected from 9 different scenes: *airport, dining hall, indoor, jail, mall, square, school, station and street*. Figure 6 shows the frame number of different scenes in HiEve. Most of these videos are selected from our own collected sequences and contain complex interactions between persons. As illustrated in the workflow in Figure 2, for each scene, we keep several videos captured at different sites and with different types of events happening to ensure

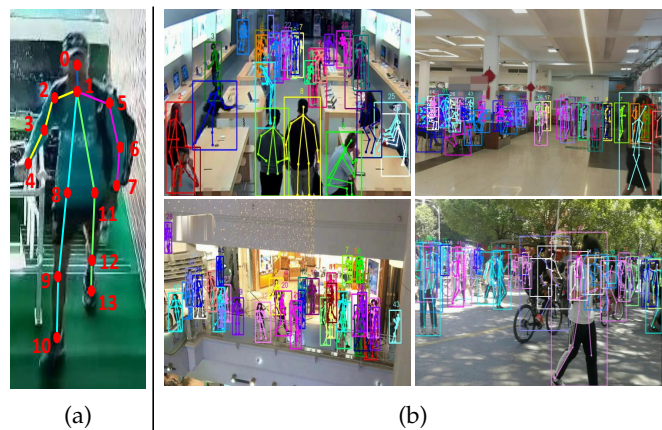


Figure 3: (a) Keypoints definition (b) Example pose and bounding-box annotations from our dataset.

the diversity of scenarios. Moreover, data redundancy is avoided through manual checking. Finally, 32 real-world video sequences in different scenes are collected, each containing one or more complex events. These video sequences are split into training and testing sets of 19 and 13 videos so that both sets cover all the scenes but with different camera angles or sites.

Annotation. In our dataset, the bounding-boxes, keypoint-based poses, human identities, and human actions are manually annotated. The annotation procedure is as follows:

First, we annotate poses for each person in the entire video. Different from PoseTrack and COCO, our annotated pose for each body contains 14 keypoints (Figure 3a): *nose, chest, shoulders, elbows, wrists, hips, knees, ankles*. Specially, we skip pose annotation which falls into any of the following conditions: (1) heavy occlusion (2) area of the bounding box is less than 500 pixels. Figure 3b presents some pose and bounding-box annotation examples.

Second, we annotate actions of all individuals every 20 frames in a video. For group actions, we assign the action label to each group member participating in this group activity. In total, we defined 14 action categories: *walking-alone, walking-together, running-alone, running-together, riding, sitting-talking, sitting-alone, queuing, standing-alone, gathering, fighting, fall-over, walking-up-down-stairs, crouching-bowing*.

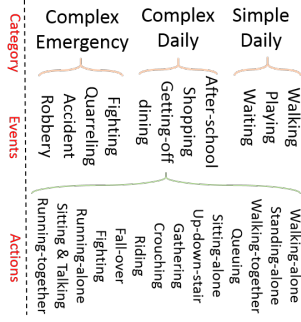


Figure 4: The classification of events. They are divided into three event categories.

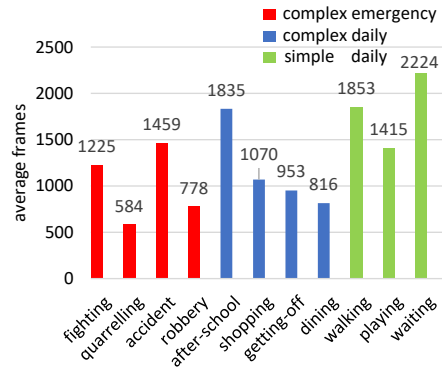


Figure 5: The distribution of events. Different colors represent different kinds of events.

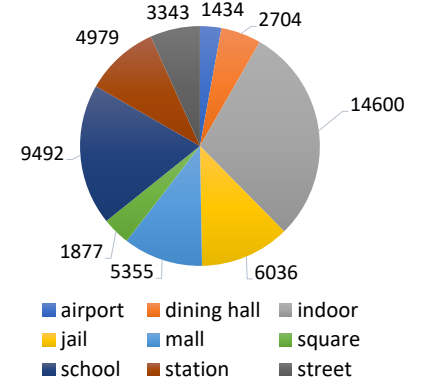


Figure 6: The frame number distribution of different scenes in HiEve dataset.

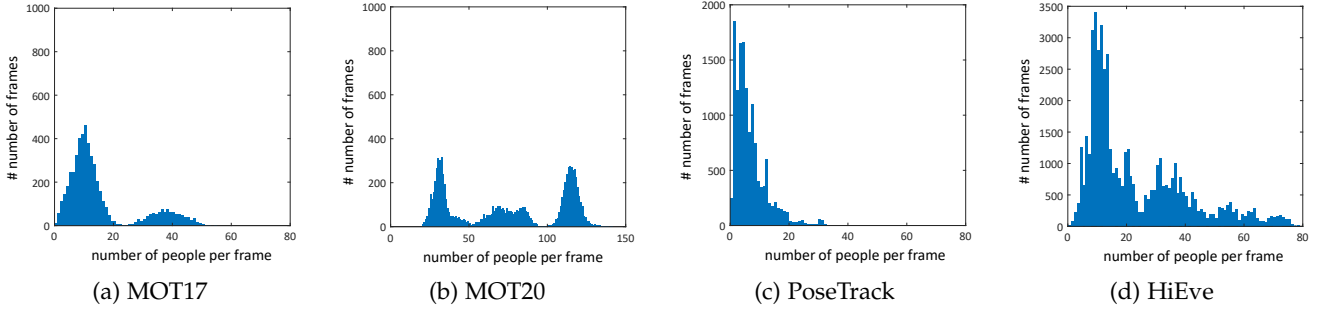


Figure 7: The distribution of the number of people per frame in MOT17, MOT20, PoseTrack and HiEve dataset. The scenes in HiEve dataset owns more people.

Figure 1 shows some samples of different actions in HiEve. *Finally*, all annotations are double-checked to ensure their quality.

3.2 HiEve Statistics

Our dataset contains 32 video sequences mostly longer than 900 frames. Their total length is 33 minutes and 18 seconds. Table 1 shows the basic statistics of our HiEve dataset: it has 49,820 frames, 1,302,481 bounding-box annotations, 2,687 track annotations, 1,099,357 human pose annotations, and 56,643 action annotations, being the largest scale human-centric dataset to our knowledge.

To further illustrate the characteristics of our dataset, we conduct the following statistical analysis.

First, we analysis some statistic information across different events. In terms of video content, we could group our video sequences into 11 **events**: *fighting, quarreling, accident, robbery, after-school, shopping, getting-off, dining, walking, playing and waiting*. Each event contains different amount of participants and action types. Then, according to the complexity of these events, we further grouped these events into 3 categories: *complex emergency event, complex daily event, and simple daily event*. The hierarchical relationship among category, events and actions is illustrated in Figure 4. We present the number of poses, objects, and tracks for the above 3 events in Figure 10, which proves that the complex events we define have more human-centric information. Moreover, Figure 5 presents the average frame number of

each event, indicating that our HiEve dataset is dominated by complex events.

Second, we present the number of people per frame in our dataset in Figure 7 demonstrating that the scenes in our video sequence have more people than MOT17 and PoseTrack [4], making our tracking task more difficult. Although MOT-20 [6] collects some video sequences with more people (up to 141 people), it only covers limited scenarios and human actions.

Third, we adopt the *Crowd Index* defined in Crowdpose [3] to measure the crowding level of our dataset. For a given frame, its Crowd Index(CI) is computed as:

$$CI = \frac{1}{n} \sum_{i=1}^n \frac{N_i^b}{N_i^a} \quad (1)$$

where n is the total number of persons in this frame. N_i^a denotes the number of joints from the i^{th} human instance and N_i^b is the number of joints located in bounding-box of the i^{th} human instance but not belonging to the i^{th} person. We evaluate the *Crowd Index* distributions of our HiEve dataset and the widely used pose dataset MSCOCO [1] and MPII [2]. Figure 9 shows that our HiEve dataset pays more attention to crowded scenes while other benchmarks are dominated by uncrowded ones. This characteristic allows the state-of-the-art methods on our dataset to cover both simple cases and ignoring crowded ones.

Fourth, we analyze the ratio of disconnected human tracks in our dataset. *Disconnected human tracks* are defined

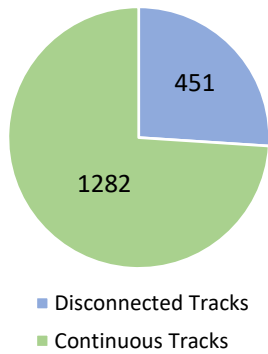


Figure 8: Number of disconnected and continuous tracks in training set.

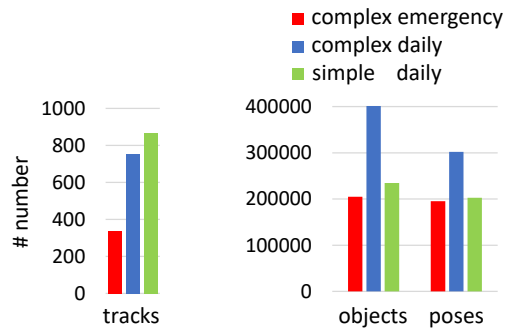


Figure 10: The number of tracks, objects and poses in events. Different colors represent different kinds of events.

as trajectory annotations where the bounding boxes are not available on some frames due to the following reasons: (1) One object temporally moves out of the camera view and moves back sometime later. (2) One object is severely occluded by foreground objects or certain obstacles for a long time so that annotators can not assign an approximate bounding box to it (as exemplified in Figure 14). It is noticeable that in datasets like PoseTrack [4], the reappearance of one individual in the scene is considered as the start of a new trajectory instead of the continuation of the original track before disappearing, in this manner these datasets will contain more tracks with shorter endurance (as reflected in Figure 11). In contrast, in HiEve we assign the tracks before and after disappearing with the same ID, so as to encourage algorithms which can properly handle long-term re-identification. The numbers of disconnected and continuous tracks in the training set are reported in Figure 8. The statistical results show that the proportion of disconnected tracks is non-negligible supporting algorithms which could handle complex cases and crowded scenes.

Finally, the distribution of all action classes in our dataset is shown in Figure 12 and could be regarded as a long-tailed sample distribution. Figure 13 demonstrates the complex events in our dataset have more concurrent events, which means that the complexity and difficulty of identifying behaviors in such scenes will increase.

Overall, these statistics further prove that HiEve is a

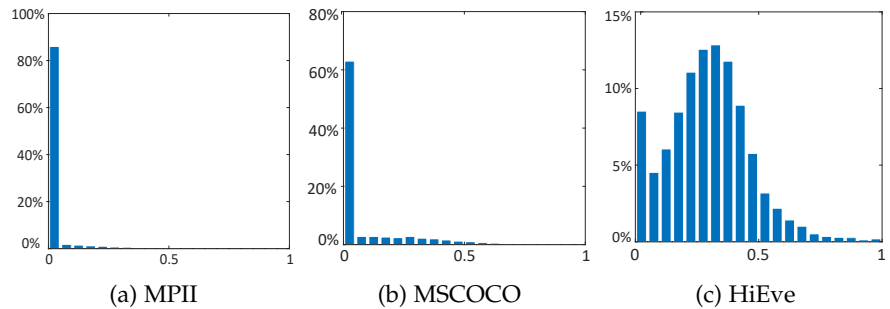


Figure 9: *CrowdIndex* distributions of MSCOCO and our HiEve dataset. MSCOCO is dominated by uncrowded images, while HiEve dataset pays more attention on crowded cases.

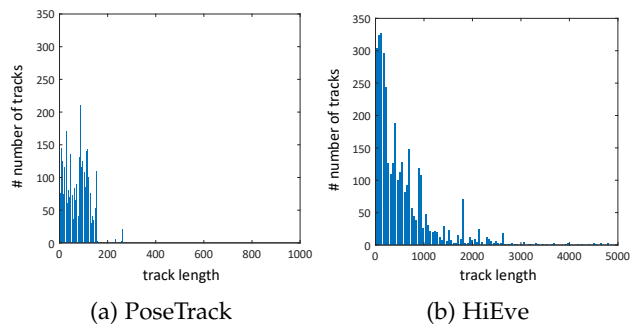


Figure 11: The distribution of the length of track in PoseTrack and HiEve dataset.

large-scale and challenging dataset dominated by complex events.

4 TASK AND METRIC

with the collected video data and available annotations, HiEve poses four tasks for the evaluation of video analysis algorithms.

Multi-person Motion Tracking. This task is proposed to estimate the location and corresponding trajectory of each identity throughout a video. Specially, we provide two sub-tracks:

- **Public:** In this sub-track, all participants can only use public object detection results provided by us, which is obtained via *Faster-RCNN* [22].
- **Private:** Participants in this sub-track are able to generate their own detection bounding-box through any approaches.

Crowd Pose Estimation. This task requires the participants to estimate specific keypoints on human skeleton. Compared with MPII Pose and MSCOCO Keypoints, our dataset involves more real-scene pose patterns in various complex events.

Crowd Pose Tracking. This task requires to provide temporally consistent poses for all people visible in the videos. Compared with PoseTrack, our dataset is much larger in scale and includes more frequent occlusions.

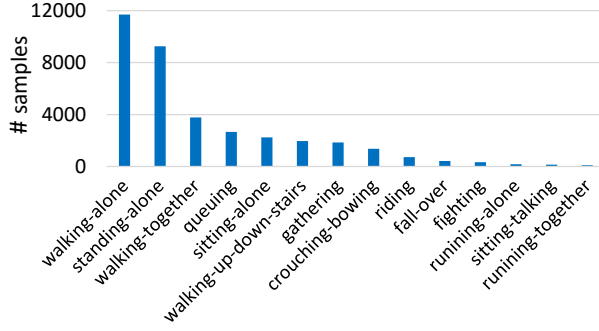


Figure 12: Sample distribution of all action classes in the HiEve dataset.

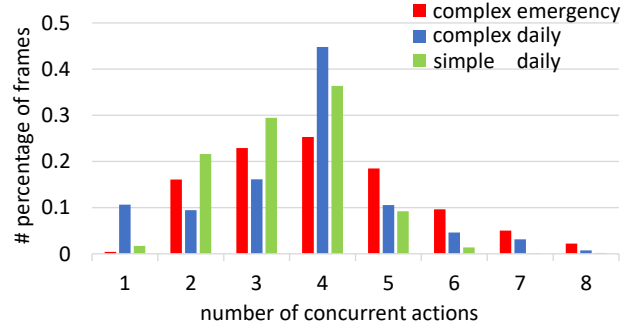


Figure 13: The distribution of the number of concurrent action in HiEve dataset. Different colors represent different kinds of events.

Person-level Action Recognition. The action recognition task requires participants to simultaneously detect specific individuals and assign correct action labels to it on every sampled frame. Compared with AVA challenge [23], our action recognition track does not only contain atomic level action definition but also involves more interactions and occlusion among individuals, making recognition more difficult.

We adopt some widely used metrics in terms of different challenge tracks, meanwhile we also design some **new metrics** to measure the performance on crowded and complex scenes.

4.1 Multi-person tracking

- **MOTA & MOTP** [5]: They are standard metrics to evaluate object tracking performance in video sequences. MOTA measures the ratio of false-positive, missing target, and identity switch. MOTP measures the trajectory similarity between predicted results and ground-truth. This measurement is adopted in the tracks of multi-person tracking and multi-person pose estimation and tracking.
- **w-MOTA**: In order to evaluate how algorithms perform on tracks with disconnected parts, we design a weighted MOTA metric (w-MOTA). This metric is computed in a similar manner as MOTA except that we assign a higher weight γ to the ID switch cases happening in disconnected tracks, consequently the metric can be formulated as

$$\mathbf{w-MOTA} = 1 - (N_{fp} + N_{fn} + N_{sw} + (\gamma - 1)N_{sw-dt}) / N_{gt}$$
 where N_{fp} and N_{fn} are the number of false positive and false negative, N_{sw} is the total times of ID switch, N_{sw-dt} is the ID switch times happening in disconnected tracks and N_{gt} is the number of bounding boxes in annotations.
- **ID F1 Score** [24]: The ratio of correctly identified detections over the average number of ground-truth and computed detections.
- **ID Sw** [24]: The total number of identity switches.
- **ID Sw-DT**: The total number of identity switches happening in disconnected tracks.

4.2 Multi-person pose estimation

- **AP@ α** We adopt *Average Precision* (AP) for measuring multi-person pose accuracy. The evaluation protocol is

similar to DeepCut [25]: First, if a pose prediction has the highest PCKh [2] (head-normalized Percentage of Correct Keypoints, where α is a distance threshold to determine whether a detected keypoint is matched to an annotated keypoint) with a certain ground-truth, then it can be assigned to the ground truth (GT). Unassigned predictions are counted as false positives. Finally, *Average Precision* (AP) is computed according to the area under the precision-recall curve.

- **w-AP@ α** To further avoid the methods only focusing on simple cases uncrowded scenarios in the dataset (although Figure 9 has shown that our dataset contains a large number of crowded and complex scenarios), we will assign larger weights to a test image during evaluation if it owns: (1) higher *Crowd Index* (2) anomalous behavior (e.g. fighting, fall-over, crouching-bowing). To be specific, the weights for the t^{th} frame in one video sequence can be formulated as:

$$w_t^P = c_1 e^{CI_t} + c_2 N_t$$

where CI_t is the crowd index on t^{th} frame calculated via Equation 1, N_t denotes the number of categories of anomalous actions. During our evaluation, the coefficients c_1, c_2 are set to 2, 1 respectively. The values of AP calculated with assigned weights are called *weighted AP* (w-AP).

- **AP@avg** We take the average value of AP@0.5, AP@0.75, and AP@0.9 as an overall measurement of keypoint estimation results, where 0.5, 0.75, and 0.9 are the specific distance threshold for computing PCKh.
- **w-AP@avg** We take the average value of w-AP@0.5, w-AP@0.75, and w-AP@0.9 as an overall measurement of keypoint estimation results on weighted video frames, where 0.5, 0.75, and 0.9 are specific distance threshold for computing PCKh.

4.3 Pose tracking

- **MOTA & MOTP** in tracking tasks are also adopted to pose tracking for evaluation.
- **AP** We calculate AP for pose tracking evaluation in the same way that introduced in the multi-person pose estimation.

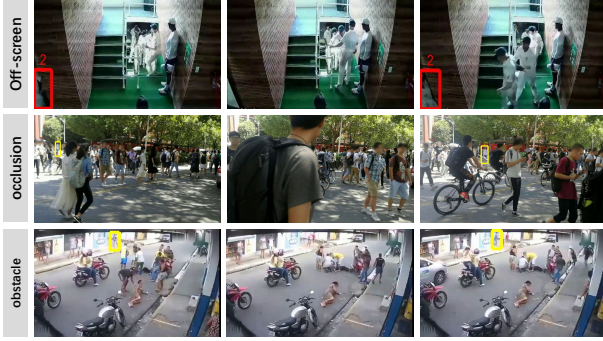


Figure 14: Examples of disconnected tracks (highlighted with bounding box)

4.4 Action recognition

- **$f\text{-mAP}@_\alpha$** The frame mAP (f-mAP) is a common metric to evaluate spatial action detection accuracy on a single frame. To be specific, each prediction consists of a bounding box and a predicted action label. If it has overlap larger than a certain threshold α with an unmatched ground-truth box of the same label, it is taken as true positive; otherwise it is a false positive. Additionally, to avoid evaluation on objects which are visually ambiguous or impossible to tell the behavior, we filter out the bounding boxes of extremely small size or severely occluded by others from annotations in the test set. Consequently, only 36% of the annotated boxes are adopted to evaluate the performance.
- **$wf\text{-mAP}@_\alpha$** Considering the unbalanced distribution of the action categories in the data set, it is appropriate to assign smaller weights to the test samples belonging to dominated categories. In addition, we assign a larger weight to frames under crowded and occluded scenarios to encourage models to perform better in complex scenes. Similar to the Weighted mAP, the frame mAP value calculated with these assigned weights is called weighted frame-mAP (wf-mAP for short)
- **$f\text{-mAP}@_{avg}$** We report f-AP@0.5, f-AP@0.6, and f-AP@0.75, where 0.5, 0.6, and 0.75 are specific IOU thresholds to determine true/false positive, and then take their mean value as an overall measurement value of f-mAP, we denote this measurement as f-mAP@avg.
- **$wf\text{-mAP}@_{avg}$** Similarly, we report wf-AP@0.5, wf-AP@0.6, and wf-AP@0.75, then take their mean value as an overall measurement value of wf-mAP, we denote this measurement as wf-mAP@avg.

5 ACTION-GUIDED POSE ESTIMATION

Skeleton-based video action recognition techniques [26], [27] have been well developed in recent years. In contrast, little attention has been paid to the potential of action information in enhancing 2D pose feature learning. Benefit from the rich and comprehensive annotations of our dataset, we build an enhanced baseline method for HiEve benchmark by guiding the pose estimation procedure with the knowledge of action types. Different from previous approaches, it introduces action information to both feature learning and refinement. As shown in Figure 16, the algorithm mainly



Figure 15: The location of key points with horizontal distribution may indicate the fall-over action. *Left*: Key-point location, *Right*: corresponding action category.

consists of two modules: action-guided domain alignment module (ADAM) and pose refinement module (PRM) module, where ADAM aligns the feature representation between the domain of action and pose, while PRM utilizes the aligned feature to refine the pose estimation results.

5.1 Action-guided domain alignment

Some special location relationships between human keypoints tend to indicate a certain anomalous behavior. For example, as illustrated in Figure 15, a human skeleton yielding a dense and horizontal keypoints distribution is usually associated with the ‘fall-over’ action. Vice versa, the action category can provide reliable prior knowledge on keypoints location. Moreover, the incorrect keypoints location could be revised by these knowledge. With this observation, we propose an action-guided domain alignment module (ADAM), where we regard the pose and action as information from two different domains. The ADAM aims at building a mapping between them, such that the two domains are close in feature space.

Follow the framework of top-down pose estimation, the pose feature \mathbf{F}_p of single person is extracted by a base convolution network. Then, an encoder \mathbf{E} with a series of down-sample operations squeezes and encodes the pose feature into a latent feature \mathbf{f}_l^p with dimension- N . To extract action information, we represent action category of the same person with a one-hot vector $\hat{\mathbf{y}}_a$, the one-hot action vector is further embedded into a latent feature \mathbf{f}_l^a through a linear transformation \mathbf{T} , with the embedded feature dimension the same as \mathbf{f}_l^p . The above process could be formulated as:

$$\mathbf{f}_l^p = \mathbf{E}(\mathbf{F}_p), \mathbf{f}_l^a = \mathbf{T}(\hat{\mathbf{y}}_a), \mathbf{f}_l^p, \mathbf{f}_l^a \in \mathbb{R}^{1 \times N}$$

where $\mathbf{T}(\cdot) = \mathbf{W}_t^2(\mathbf{W}_t^1(\cdot))$, $\mathbf{W}_t^2 \in$ and \mathbf{W}_t^1 are parameters of two fully-connected layers.

Finally, an alignment loss is calculated between latent features from two domains, which aims at encouraging feature consistency between them by minimizing their Euclidean distance in the latent space.

$$\mathcal{L}_{align} = \text{MSE}(\mathbf{f}_l^p, \mathbf{f}_l^a)$$

5.2 Pose refinement

To further improve the quality of pose estimation, we design a refinement module based on the latent pose features, which comprises two head structures: spatial refinement head (SR) and channel-wise refinement head (CR).

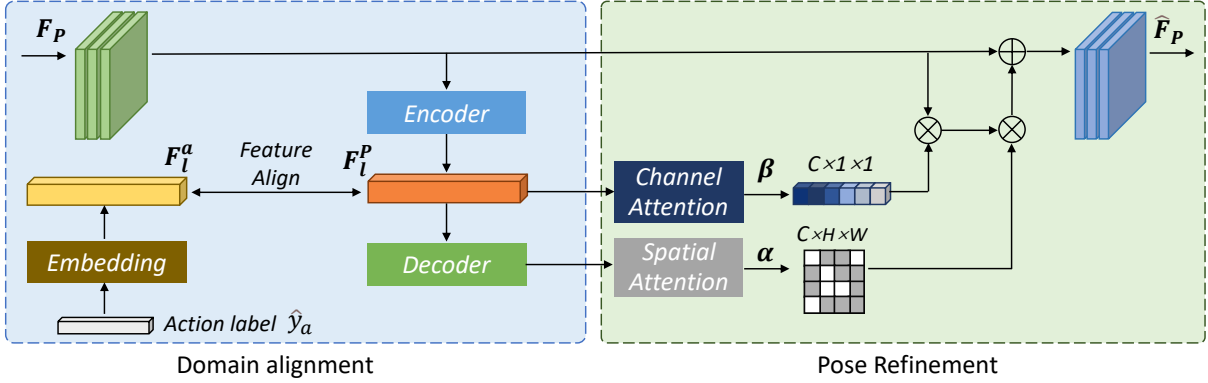


Figure 16: The framework of our algorithm.

In pose estimation, the position of keypoints is reflected by the local responses in the spatial feature maps. Therefore, the SR intends to re-weight the spatial feature map by emphasizing specific skeleton position and suppressing inaccurate keypoints response. Corresponding to the encoder in ADAM, the SR applies an decoder, which consists of a series of up-sampling operations to output an attention mask α from \mathbf{f}_p :

$$\alpha = \sigma(\mathbf{W}_s^1(\mathbf{D}(\mathbf{f}_l^p)))$$

where $\mathbf{W}_s^1 \in \mathbb{R}^{N \times N}$ are the parameters of a depth-wise separable 9×9 convolution, the output attention map α implicitly contains the keypoints prior from action-specific knowledge. On the other hand, inspired by the SENet [28], the CR aims at performing channel-wise feature re-calibration in a global sense, where the per-channel summary statistics are utilized to selectively emphasis informative feature maps as well as suppress useless ones. To be specific, the latent feature passes through two fully-connected layers and a sigmoid activation to obtain an attention vector β for each channel

$$\beta = \sigma(\mathbf{W}_c^2 \cdot \delta(\mathbf{W}_c^1 \mathbf{f}_l^p))$$

where $\sigma(\cdot)$ and δ represent the sigmoid and ReLU functions respectively, $\mathbf{W}_c^1 \in \mathbb{R}^{d \times N}$ and $\mathbf{W}_c^2 \in \mathbb{R}^{N \times N}$ refer two fully-connection layers.

The channel-wise and spatial attention guidance is then applied to refine pose feature as

$$\hat{\mathbf{F}}_p = \mathbf{F}_p \otimes (1 + \beta \otimes \alpha)$$

5.3 Implementation Details

The HRNet [29] pretrained on COCO is chosen as our backbone for pose feature extraction training. The proposed modules are appended after the last stage of HRNet. Our *Encoder* and *Decoder* use the corresponding downsample and upsample architecture in U-Net, respectively. For *training*, the whole network is trained on the HiEve training set. For a fair comparison, same as we described in 6.2, we take the YOLO v3 as person detector. As the actions are annotated every 20 frames in HiEve, we utilize interpolation to create action category labels for all individuals in every frame. We set different learning rates for the backbone HRNet and our proposed modules, which are $1e-4$ and $1e-3$ respectively. In our experiments, we will show that our model gains the

ability of mining potential action information to refine the poses. During training phase, the total loss for training is defined as:

$$\mathcal{L} = \mathcal{L}_{reg} + \mathcal{L}_{align}$$

where the \mathcal{L}_{reg} is the traditional heatmap regression L2 loss. During inference, the action label embedding process is removed, and the proposed modules are connected with the last stage's output of HRNet.

6 EXPERIMENTS AND RESULTS

6.1 Multi-person tracking

Baselines

- DeepSORT [30]. Based on the SORT [36] algorithm, it introduces an offline model pre-trained on person re-ID datasets. In real-time object tracking, appearance features are extracted by the pre-trained model, and simple nearest neighbor query is performed to track pedestrians.
- MOTDT [31]. MOTDT tackles unreliable detection by selecting candidates from outputs of both detection and tracks. Besides, A new scoring function for candidate selection is formulated by an efficient R-FCN, which shares computations on the entire image.
- IOUtracker [32]. IOUtracker proposes a very simple and efficient tracking algorithm, which only leverages the detection results and designs an IOU strategy to improve the performance of multi-objective tracking.
- JDE [33]. JDE Tracker is the first joint pipeline for simultaneous detection and tracking, which produce the object embedding to accosiate persons across frames.
- FairMOT [34]. FairMOT is another joint detection-tracking pipeline, which focuses on addressing spatial misalignment with under an anchor-free manner.

Implementation Details

Faster R-CNN [22] is used to obtain the public results of bounding-boxes firstly. In MOTDT and DeepSORT, we use the train set of HiEve and the ground truth to fine-tune the official deep models in these methods. Then, we evaluate them in the HiEve test dataset with the public detection results. The threshold of detections is set to be 0.2.

Results and Analysis

The results of these three baselines are shown in Table 2 and Figure 17. We can observe that all three methods

Table 2: Results of multi-person tracking baselines.

Method	MOTA	w-MOTA	MOTP	IDF1	MT	ML	FP	FN	IDS _w	IDS _w -DT
DeepSORT [30]	27.12	21.95	70.47	28.55	8.50%	41.45%	5894	42668	2220	90
MOTDT [31]	26.09	21.73	76.50	32.88	8.70%	54.56%	6318	43577	1599	76
IOUtracker [32]	38.59	33.31	76.23	38.62	28.33%	27.60%	9640	28993	4153	92
JDE [33]	33.12	27.78	72.27	36.01	15.11%	24.13%	9526	33327	3747	93
FairMOT [34]	35.03	30.49	75.57	46.65	16.26%	44.18%	6523	37750	995	79

Table 3: Results of multi-person pose estimation. ‘FT’ means the model has been fine-tuned on HiEve training set with the same setting as our algorithm.

Method	w-AP@avg	w-AP@0.5	w-AP@0.75	w-AP@0.9	AP@avg	AP@0.5	AP@0.75	AP@0.9
HRNet [29]	47.12	53.66	46.42	41.28	50.72	57.10	50.11	44.95
Simple Baseline [35]	41.36	47.67	40.73	35.68	44.56	50.84	43.85	38.98
RMPE [9]	49.56	57.85	47.90	42.92	53.26	61.26	51.69	46.84
FT-HRNet	51.88	59.67	50.69	45.58	55.68	63.11	54.33	49.61
FT-Simple Baseline	50.59	59.00	48.98	43.80	54.51	62.82	52.90	47.81
Ours	53.95	63.02	52.16	46.68	57.67	66.48	55.94	50.60

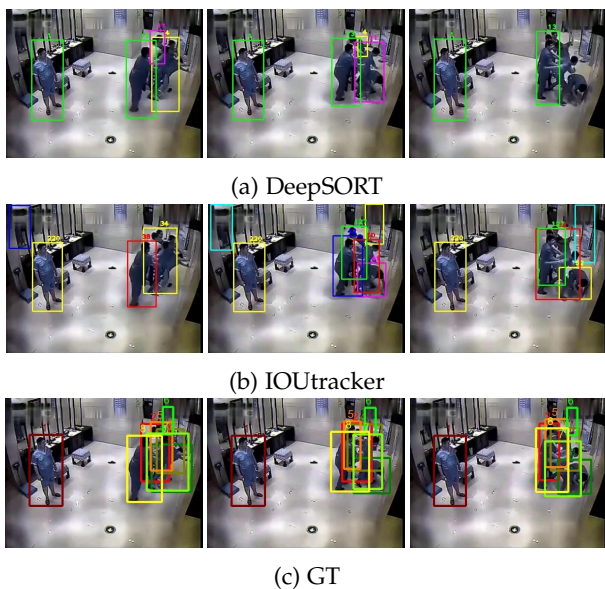


Figure 17: Visualized results of MOT baselines and the ground-truth (GT).

perform poorly on our dataset. This is because our dataset has complex scenes and a large number of overlapping targets, making identification and tracking more difficult. IOUtracker performs best on our dataset, while MOTDT [31] and DeepSORT [30] have a relatively worse performance. Meanwhile, the joint detection-and-tracking solution [33], [34] also perform worse than simple IOU Tracker. The reason is that our dataset contains a large number of crowded scenes and occlusions, so it is hard for either ReID or backbone model to extract representative features to distinguish different object instances.

6.2 Multi-pose estimation

Baselines

- RMPE [9]. RMPE designs a new symmetric spatial transformer network (SSTN) to transform and correct the inaccurate object localization. Besides, pose NMS is proposed to solve the problem of redundant human detections.

- Simple-Baseline [35]. It improve the ResNet [37] by adding a few deconvolutional layers. Extensive experiments show that it’s a simple and strong baseline for pose estimation and tracking.
- HRNet [29]. HRNet aims to learn reliable high-resolution representations for pose estimation. Specifically, the high-to-low resolution subnetworks are added one by one to form more stages, and multi-resolution subnetworks are connected in parallel.
- Our Algorithm. Our proposed pose estimation algorithm, which utilizes the action category label as an auxiliary information to refine the human pose feature learning.

Implementation Details

For the above top-down methods, we take the detection results of YOLO v3 [38] as their input. All the performance is reported using their official codes and models. In HRNet, the HRNet-32 model pre-trained on MPII [2] is selected to be the backbone with input object size 256. For Simple Baseline, we use ResNet-50 [37] model pre-trained on MPII and adopt flip strategy for testing. In RMPE, SPPE [39] is the backbone during testing. For the sake of fair comparison, we also fine-tune the COCO pre-trained HRNet and Simple Baseline on our HiEve training set with the same setting as our algorithm, their performances are reported as well. More implementation details of our algorithm could refer to [subsection 5.3](#).

Results and Analysis

We present the evaluation results in [Table 3](#) and the visualization results in [Figure 18](#). Before fine-tuning on HiEve dataset, RMPE [9] performs best on our dataset although the HRNet is recognized as the state-of-the-art method. The reason might be that HRNet is more susceptible to the quality of detection boxes while the STN module in RMPE is able to correct inaccurate detection results. After fine-tuning in our HiEve dataset, w-AP of HRNet and the Simple baseline are further boosted by 4.76 and 9.23. However, our proposed algorithm still outperforms these two powerful baselines by 2.07 and 3.36 w-AP on HiEve dataset respectively. The comparisons manifest that by introducing action category information, the pose estimation network with aligned feature and attention mechanism could generate more accurate keypoints location in crowded scenes.

Table 4: Results of action recognition baselines.

Method	wf-mAP				f-mAP			
	avg	0.5	0.6	0.75	avg	0.5	0.6	0.75
Threshold	6.88	9.65	7.91	3.07	8.31	11.01	9.65	4.26
RPN+I3D [40]	10.13	13.35	11.57	5.49	10.95	14.50	12.33	6.01
Faster R-CNN+I3D [22]	7.28	9.88	8.32	3.65	7.03	9.32	8.10	3.66
Transformer+I3D [41]	5.29	6.76	6.39	2.71	7.37	8.53	9.00	4.58

Table 5: Results of pose tracking baselines.

Method	MOTA	MOTP	AP
RMPE + PoseFlow [43]	44.17	48.33	60.10
LightTrack [44]	27.44	55.23	29.36
Ours + PoseFlow	45.36	49.97	63.16

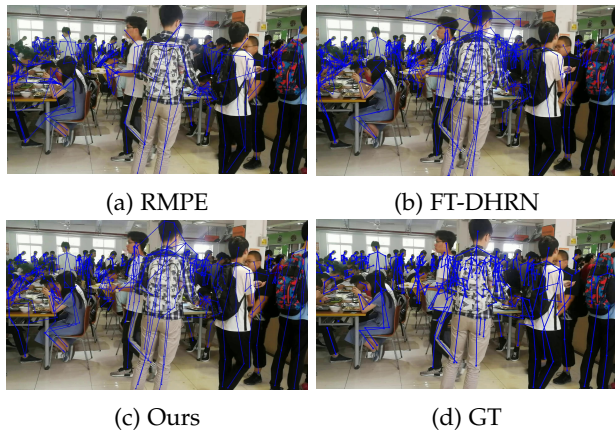


Figure 18: Visualized results of pose estimation baselines and the ground-truth (GT).

6.3 Pose tracking

Baselines

- PoseFlow [43]. It’s an efficient pose tracker based on flows and top-down approaches RMPE [9]. An online optimization framework is designed to build the association of cross-frame poses and form pose flows (PF-Builder). Then, a novel pose flow non-maximum suppression (PF-NMS) is designed to robustly reduce redundant pose flows and re-link temporal disjoint ones.
- LightTrack [44]. LightTrack is an effective light-weight framework for online human pose tracking. It unifies single-person pose tracking with multi-person identity association.
- Our method + PoseFlow. Based on the pose estimation results of our algorithm, we adapted PoseFlow method to conduct human pose tracking across frames.

Implementation Details

In LightTrack, *YOLO v3*, Siamese GCN, and MobileNet are selected as the keyframe detector, ReID module, and pose estimator respectively. We use DeepMatching to extract dense correspondences between adjacent frames in PoseFlow. All weights of model inherit from pre-trained models on MSCOCO [1].

Results and Analysis

The performance comparison of these three methods is presented in Table 5. As expected, the flow-based algorithm PoseFlow achieves higher performance while Light-

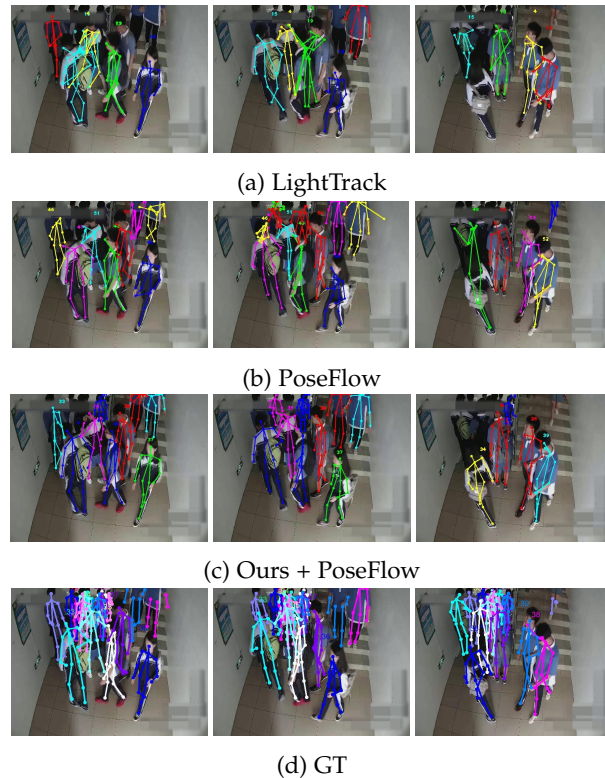


Figure 19: Visualized results of pose tracking baselines and the ground-truth (GT).

Track [44] mainly aims to strike a balance between speed and accuracy. The Figure 19 shows the visualization results of them, PoseFlow is able to track more people than LightTrack, but they all face the issue of losing objects and bad keypoints localization in crowded scenes. Enhanced by the accurate keypoints location of our proposed pose estimation algorithm, the performance of PoseFlow could be further improved.

6.4 Action recognition

Baselines

- RPN+I3D [40]. In this method, the I3D [45] network is applied for feature extraction and classification, and the feature from the labelled key-frame is fed to RPN [22] for region proposal.
- Faster R-CNN+I3D. We further improve the baseline in [40] for better localization. To be specific, we do not predict region directly on the I3D feature, instead, an independent Faster R-CNN detector [22] is applied on the input key-frame to obtain the bounding box proposals.
- Video Transformer Network [41]. The Video Transformer Network (VTN) takes the I3D network as backbone and

applies a key-value attention mechanism to model the interaction among objects before the classification layer to improve recognition results.

- SlowFast [42]. The SlowFast model involves two pathway, the slow pathway operates at low frame rate, to capture spatial semantics, and the fast pathway operates at high frame rate, to capture motion at fine temporal resolution.

Implementation Details

For all baselines except for SLOWFast [42], we adopt the RGB-I3D [45] network with Inception-V1, initialized with Kinetics-pretrained weights, as a video feature extractor. The SlowFast takes pretrained inflated-ResNet50 [46] as backbone. In RPN+I3D, following [40], we generate region proposals by RPN on key-frame feature and implement action classification and box regression with I3D head. In Faster R-CNN+I3D and SlowFast, we use detection results of a Faster R-CNN detector as ROIs and perform action classification on ROI aligned features. In VTN, we use the same Faster R-CNN detection results as ROIs, but employ the transformer head in [41] for action classification. For all experiments, we fix the statistics of batch norm layers.

Results and Analysis

The main results are shown in Table 4. The model employing I3D [45] with Faster R-CNN detector performs best on our dataset, outperforming that using I3D for both detection and classification. It’s probably because our dataset contains a large number of crowded scenes, which is challenging for detection. Therefore, utilizing a high-quality detector could significantly improve the detection performance. The method with transformer is superior on AVA [21] dataset but performs comparatively poor on our dataset, the reason might be that AVA dataset focuses on human-human and human-object interaction, while our dataset pays more attention to the individual action under complex event conditions. Surprisingly, the state-of-the-art method SlowFast performs the worst in our dataset. This result may be related to the crowded and severe occlusion in our dataset, which makes the fast pathway in SlowFast fail in capturing motion features of individuals. Moreover, the visualization results of first three baselines are shown in Figure 20, we can observe that it’s difficult for these popular methods to recognize the anomalous actions in our dataset and none of them can tackle the prediction in crowded scenes well.

7 MORE ANALYSIS AND ABLATION STUDY

In this section, we first conduct experiments to analyze the characteristics of our HiEve dataset. Then, the ablation studies of our proposed algorithm will be presented to evaluate different variants of our proposed algorithm.

7.1 Experimental characteristics

Group & fine-grained action First, to better understand the difficulty of action recognition on the HiEve, we calculate the per-class AP value for each action category. Figure 21 displays the results obtained by SlowFast [42] method. What stands out in this figure is the poor performance of some group behavior recognition, such as ‘gathering’, ‘running-together’, and ‘sitting-talking’. Besides, the performance encounters a marked decline when recognizing fine-grained

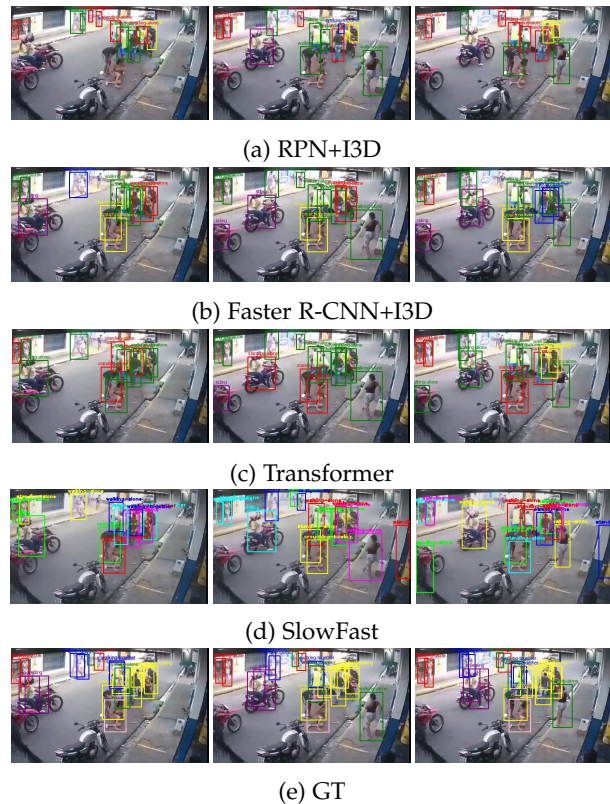


Figure 20: Visualized results of action recognition baselines and the ground-truth (GT).

actions. For example, the algorithm is hard to distinguish the ‘running-alone’ from ‘sitting-alone’. These results suggest that some measures could be taken to tackle the group and fine-grained action recognition problem in our HiEve dataset for further improvement.

Hard video sequence First, we make a simple subjective analysis of the test video sequence. The *CrowdIndex* is calculated for each test video sequence to measure the crowding level of frames. The top-3 sequences with the highest *CrowdIndex* could be naturally regarded as relatively hard examples in the test set. Specifically, they are *hm_in_bus* (ID:21), *hm_in_dining_room2* (ID:22), and *hm_in_subway_station* (ID:24). Furthermore, we report the weighted-AP of FT-HRNet[29] on each video sequence, since this metric pays more attention to crowded scenarios. As shown in Figure 22, consistent with our assumption, the performance shows a sharp degradation in all of these three video sequences. This indicates that the crowded level is a major influence on video understanding tasks in HiEve. Surprisingly, the performance on video sequence *hm_in_stair3* (ID:30) also meets a marked drop whereas its crowded level is relatively low among all sequences. The reason for this is that it was dominated by the overhead view. To sum up, the hard example in our data set are close to the real-world scenes, namely, the severe human occlusion and various video angles.

Upper bound test All the human-centric video understanding tasks are tightly associated with object detection. To study the impact of detection accuracy in the HiEve dataset, we conduct the upper bound test on each task with

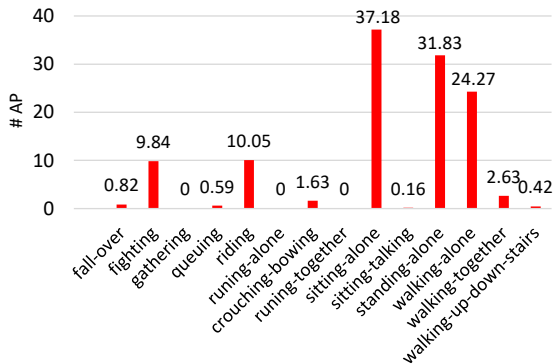


Figure 21: The performance of SlowFast on each action category in HiEve

Table 6: Results of breakdown modules of our algorithm on HiEve dataset. \checkmark means the module is used

Modules		Performance	
ADAM	PRM	w-AP@avg	AP@avg
		51.88	55.68
\checkmark		53.52	65.93
\checkmark	\checkmark	53.95	66.48

Table 8: The upper bound and normal setting results for each track

Track	Methods	Normal	Oracle
1-human tracking	IOUTracker[32]	MOTA	
		38.59	97.70
2-pose estimation	FT-HRNet[29]	w-AP@avg	
		51.88	53.342
3-pose tracking	PoseFlow[43]	MOTA	
		44.17	73.84
4-action recognition	SlowFast[42]	f-mAP@avg	
		5.29	13.21

Table 9: Downstream task results with and without HiEve pretraining

Pretraining ?	Downstream task	
	HRNet [29] on COCO	MOTD [31] on MOT20
NO	74.4	46.4
YES	74.8	47.6

specific oracle models, where the ground-truth bounding-boxes are directly used during testing, including multi-person tracking, pose estimation, and action recognition. We compared them with the normal setting that we described in section 6 without ground-truth. Table 8 lists the upper bound results for each track. It suggests that the tasks requiring temporal reasoning (Track1&3&4) rely more on the accuracy of the detection. In contrast, the pose estimation track is more dependent on the corresponding algorithm than the detection results.

Ability for knowledge transfer. HiEve covers large amounts of video frame data with a wide range of human-centric annotations, making it well suitable for model pre-training to inject these models with more comprehensive prior knowledge on downstream tasks. To demonstrate this characteristics, we conduct experiments on transfer learning

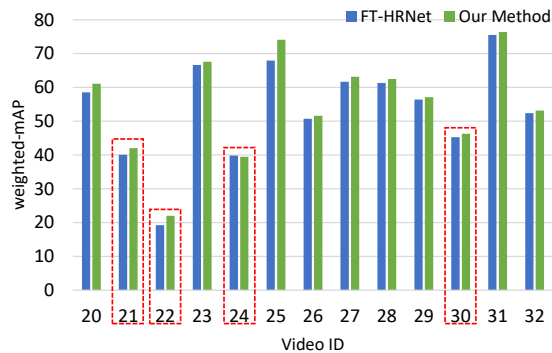


Figure 22: The performance of FT-HRNet on each video sequence in HiEve. Hard video examples (weighted-AP \leq 50) are emphasized by red dashed boxes.

Table 7: Results by different refinement configurations on HiEve dataset

Refinement Setting		Performance	
SR	CR	w-AP@avg	AP@avg
\checkmark		51.67	60.43
	\checkmark	53.69	66.25
\checkmark	\checkmark	53.95	66.48

from HiEve to other two related downstream tasks, human pose estimation and multiple object tracking. In detail, we apply HRNet [29] for pose estimation on COCO [1] and MOTDT [31] on MOT20 [6]. For each task, we compare the results with and without pretraining on our HiEve datasets in Table 9. For COCO we report the average AP value, for MOT20 we report the MOTA metric. It is observed that for both downstream task, pretraining on HiEve can help improve the methods obtain better performance.

7.2 Ablation study of our algorithm

The contributions of different modules in our model are first analyzed via experiments. Table 6 presents the breakdown results of the action-guided domain alignment (ADAM) and pose refinement module (PRM). We can observe that by introducing action category information as a kind of regularization, the performance can achieve a large improvement of 1.64 weighted-AP. Besides, the performance can be further boosted to 53.95 w-AP with the refinement module, which indicates that the attention mask generated by the aligned latent feature fosters the pose feature revision and refinement.

To further validate the effectiveness of the PRM, we apply the SR and CR separately. As shown in Table 7, each refinement plays an important role in the final performance. The application of single SR module gains 4.75 AP from the vanilla HRNet. One unanticipated result is that the w-AP slightly falls, which may be due to the difficulty of spatial attention modeling for severe occlusion scenes. With the combination of CR, the refinement module could provide the best performance improvement. This experiment demonstrates that the channel-wise refinement contributes more significantly to pose estimation refinement in crowded scenarios.

8 CONCLUSION

We present HiEve, a large-scale dataset for human-centric video analysis. The HiEve dataset covers a wide range of crowded scenes and complex events. We report the results of plenty of approaches in our dataset. Extensive experiments show that the HiEve is a challenging dataset for pose estimation, pose tracking, multi-person tracking, and action recognition. Based on this dataset, we propose an action-guided pose estimation algorithm, which guides the pose representation learning with additional action information. Experiments demonstrate that it's able to boost the performance of existing state-of-the-art pipelines on our HiEve dataset.

REFERENCES

- [1] T.-Y. Lin, M. Maire, S. Belongie, J. Hays, P. Perona, D. Ramanan, P. Dollár, and C. L. Zitnick, "Microsoft coco: Common objects in context," in *European conference on computer vision*. Springer, 2014, pp. 740–755.
- [2] M. Andriluka, L. Pishchulin, P. Gehler, and B. Schiele, "2d human pose estimation: New benchmark and state of the art analysis," in *Proceedings of the IEEE Conference on computer Vision and Pattern Recognition*, 2014, pp. 3686–3693.
- [3] J. Li, C. Wang, H. Zhu, Y. Mao, H.-S. Fang, and C. Lu, "Crowdpose: Efficient crowded scenes pose estimation and a new benchmark," in *Proceedings of the IEEE Conference on Computer Vision and Pattern Recognition*, 2019, pp. 10 863–10 872.
- [4] M. Andriluka, U. Iqbal, E. Insafutdinov, L. Pishchulin, A. Milan, J. Gall, and B. Schiele, "Posetrack: A benchmark for human pose estimation and tracking," in *Proceedings of the IEEE Conference on Computer Vision and Pattern Recognition*, 2018, pp. 5167–5176.
- [5] A. Milan, L. Leal-Taixé, I. Reid, S. Roth, and K. Schindler, "Mot16: A benchmark for multi-object tracking," *arXiv preprint arXiv:1603.00831*, 2016.
- [6] P. Dendorfer, H. Rezatofighi, A. Milan, J. Shi, D. Cremers, I. Reid, S. Roth, K. Schindler, and L. Leal-Taixé, "Mot20: A benchmark for multi object tracking in crowded scenes," *arXiv preprint arXiv:2003.09003*, 2020.
- [7] C. Lu, J. Shi, and J. Jia, "Abnormal event detection at 150 fps in matlab," in *Proceedings of the IEEE international conference on computer vision*, 2013, pp. 2720–2727.
- [8] W. Sultani, C. Chen, and M. Shah, "Real-world anomaly detection in surveillance videos," in *Proceedings of the IEEE Conference on Computer Vision and Pattern Recognition*, 2018, pp. 6479–6488.
- [9] H.-S. Fang, S. Xie, Y.-W. Tai, and C. Lu, "Rmpe: Regional multi-person pose estimation," in *Proceedings of the IEEE International Conference on Computer Vision*, 2017, pp. 2334–2343.
- [10] V. Veeriah, N. Zhuang, and G.-J. Qi, "Differential recurrent neural networks for action recognition," in *Proceedings of the IEEE international conference on computer vision*, 2015, pp. 4041–4049.
- [11] X. Shu, J. Tang, G. Qi, W. Liu, and J. Yang, "Hierarchical long short-term concurrent memory for human interaction recognition," *IEEE transactions on pattern analysis and machine intelligence*, 2019.
- [12] J. Ferryman and A. Shahrokni, "Pets2009: Dataset and challenge," in *2009 Twelfth IEEE international workshop on performance evaluation of tracking and surveillance*. IEEE, 2009, pp. 1–6.
- [13] A. Geiger, P. Lenz, and R. Urtasun, "Are we ready for autonomous driving? the kitti vision benchmark suite," in *2012 IEEE Conference on Computer Vision and Pattern Recognition*. IEEE, 2012.
- [14] S. Johnson and M. Everingham, "Clustered pose and nonlinear appearance models for human pose estimation." in *bmvc*, vol. 2, no. 4. Citeseer, 2010, p. 5.
- [15] B. Sapp and B. Taskar, "Modec: Multimodal decomposable models for human pose estimation," in *Proceedings of the IEEE Conference on Computer Vision and Pattern Recognition*, 2013, pp. 3674–3681.
- [16] M. Eichner and V. Ferrari, "We are family: Joint pose estimation of multiple persons," in *European conference on computer vision*. Springer, 2010, pp. 228–242.
- [17] M. Fabbri, F. Lanzi, S. Calderara, A. Palazzi, R. Vezzani, and R. Cucchiara, "Learning to detect and track visible and occluded body joints in a virtual world," in *Proceedings of the European Conference on Computer Vision (ECCV)*, 2018, pp. 430–446.
- [18] J. Carreira and A. Zisserman, "Quo vadis, action recognition? a new model and the kinetics dataset," in *proceedings of the IEEE Conference on Computer Vision and Pattern Recognition*, 2017, pp. 6299–6308.
- [19] K. Soomro, A. R. Zamir, and M. Shah, "Ucf101: A dataset of 101 human actions classes from videos in the wild," *arXiv preprint arXiv:1212.0402*, 2012.
- [20] W. Kay, J. Carreira, K. Simonyan, B. Zhang, C. Hillier, S. Vijayanarasimhan, F. Viola, T. Green, T. Back, P. Natsev, M. Suleyman, and A. Zisserman, "The kinetics human action video dataset," 2017.
- [21] C. Gu, C. Sun, D. A. Ross, C. Vondrick, C. Pantofaru, Y. Li, S. Vijayanarasimhan, G. Toderici, S. Ricco, R. Sukthankar *et al.*, "Ava: A video dataset of spatio-temporally localized atomic visual actions," in *Proceedings of the IEEE Conference on Computer Vision and Pattern Recognition*, 2018, pp. 6047–6056.
- [22] S. Ren, K. He, R. Girshick, and J. Sun, "Faster r-cnn: Towards real-time object detection with region proposal networks," *IEEE Transactions on Pattern Analysis and Machine Intelligence*, vol. 39, no. 6, pp. 1137–1149, 2017.
- [23] C. Gu, C. Sun, S. Vijayanarasimhan, C. Pantofaru, D. A. Ross, G. Toderici, Y. Li, S. Ricco, R. Sukthankar, C. Schmid, and J. Malik, "Ava: A video dataset of spatio-temporally localized atomic visual actions," *CVPR*, pp. 6047–6056, 2018.
- [24] E. Ristani, F. Solera, R. Zou, R. Cucchiara, and C. Tomasi, "Performance measures and a data set for multi-target, multi-camera tracking," in *European Conference on Computer Vision*. Springer, 2016, pp. 17–35.
- [25] L. Pishchulin, E. Insafutdinov, S. Tang, B. Andres, M. Andriluka, P. V. Gehler, and B. Schiele, "Deepcut: Joint subset partition and labeling for multi person pose estimation," in *Proceedings of the IEEE conference on computer vision and pattern recognition*, 2016.
- [26] J. Liu, G. Wang, L.-Y. Duan, K. Abdiyeva, and A. C. Kot, "Skeleton-based human action recognition with global context-aware attention lstm networks," *IEEE Transactions on Image Processing*, vol. 27, no. 4, pp. 1586–1599, 2017.
- [27] Y. Du, Y. Fu, and L. Wang, "Representation learning of temporal dynamics for skeleton-based action recognition," *IEEE Transactions on Image Processing*, vol. 25, no. 7, pp. 3010–3022, 2016.
- [28] J. Hu, L. Shen, and G. Sun, "Squeeze-and-excitation networks," in *Proceedings of the IEEE Conference on Computer Vision and Pattern Recognition (CVPR)*, June 2018.
- [29] J. Wang, K. Sun, T. Cheng, B. Jiang, C. Deng, Y. Zhao, D. Liu, Y. Mu, M. Tan, X. Wang, W. Liu, and B. Xiao, "Deep high-resolution representation learning for visual recognition," *IEEE transactions on pattern analysis and machine intelligence*, vol. PP, April 2020.
- [30] N. Wojke, A. Bewley, and D. Paulus, "Simple online and realtime tracking with a deep association metric," in *2017 IEEE international conference on image processing (ICIP)*. IEEE, 2017, pp. 3645–3649.
- [31] L. Chen, H. Ai, Z. Zhuang, and C. Shang, "Real-time multiple people tracking with deeply learned candidate selection and person re-identification," in *2018 IEEE International Conference on Multimedia and Expo (ICME)*. IEEE, 2018, pp. 1–6.
- [32] E. Bochinski, V. Eiselein, and T. Sikora, "High-speed tracking-by-detection without using image information," in *2017 14th IEEE International Conference on Advanced Video and Signal Based Surveillance (AVSS)*. IEEE, 2017, pp. 1–6.
- [33] Z. Wang, L. Zheng, Y. Liu, and S. Wang, "Towards real-time multi-object tracking," *arXiv preprint arXiv:1909.12605*, 2019.
- [34] Y. Zhang, C. Wang, X. Wang, W. Zeng, and W. Liu, "Fairmot: On the fairness of detection and re-identification in multiple object tracking," *arXiv preprint arXiv:2004.01888*, 2020.
- [35] B. Xiao, H. Wu, and Y. Wei, "Simple baselines for human pose estimation and tracking," in *Proceedings of the European conference on computer vision (ECCV)*, 2018, pp. 466–481.
- [36] A. Bewley, Z. Ge, L. Ott, F. Ramos, and B. Upcroft, "Simple online and realtime tracking," in *2016 IEEE International Conference on Image Processing (ICIP)*. IEEE, 2016, pp. 3464–3468.
- [37] K. He, X. Zhang, S. Ren, and J. Sun, "Deep residual learning for image recognition," in *Proceedings of the IEEE conference on computer vision and pattern recognition*, 2016, pp. 770–778.
- [38] J. Redmon and A. Farhadi, "Yolov3: An incremental improvement," *arXiv*, 2018.
- [39] A. Newell, K. Yang, and J. Deng, "Stacked hourglass networks for human pose estimation," in *European conference on computer vision*. Springer, 2016, pp. 483–499.

- [40] R. Girdhar, J. Carreira, C. Doersch, and A. Zisserman, "A better baseline for ava," *arXiv preprint arXiv:1807.10066*, 2018.
- [41] —, "Video action transformer network," in *Proceedings of the IEEE Conference on Computer Vision and Pattern Recognition*, 2019, pp. 244–253.
- [42] C. Feichtenhofer, H. Fan, J. Malik, and K. He, "Slowfast networks for video recognition," in *ICV*, 2019, pp. 6202–6211.
- [43] Y. Xiu, J. Li, H. Wang, Y. Fang, and C. Lu, "Pose flow: Efficient online pose tracking," *arXiv preprint arXiv:1802.00977*, 2018.
- [44] G. Ning and H. Huang, "Lighttrack: A generic framework for online top-down human pose tracking," *arXiv preprint arXiv:1905.02822*, 2019.
- [45] J. Carreira and A. Zisserman, "Quo vadis, action recognition? a new model and the kinetics dataset," *2017 IEEE Conference on Computer Vision and Pattern Recognition (CVPR)*, Jul 2017.
- [46] X. Wang, R. Girshick, A. Gupta, and K. He, "Non-local neural networks," in *CVPR*, 2018.